Dual black holes in merger remnants – II. Spin evolution and gravitational recoil

M. Dotti,[1,2]⋆ M. Volonteri,[1] A. Perego,[3,4] M. Colpi,[4] M. Ruszkowski[1,5] and F. Haardt[2,6]

[1]*Department of Astronomy, University of Michigan, Ann Arbor, MI 48109, USA*
[2]*Dipartimento di Fisica e Matematica, Università dell'Insubria, Via Valleggio 11, 22100 Como, Italy*
[3]*Department of Physics, University of Basel, Klingerbergstr. 82, 4056 Basel, Switzerland*
[4]*Dipartimento di Fisica G. Occhialini, Università degli Studi di Milano Bicocca, Piazza della Scienza 3, 20126 Milano, Italy*
[5]*The Michigan Centre for Theoretical Physics, Ann Arbor, MI 48109, USA*
[6]*INFN, Sezione di Milano–Bicocca, 20126 Milano, Italy*

ABSTRACT

Using high-resolution hydrodynamical simulations, we explore the spin evolution of massive dual black holes orbiting inside a circumnuclear disc, relic of a gas-rich galaxy merger. The black holes spiral inwards from initially eccentric co- or counter-rotating coplanar orbits relative to the disc's rotation, and accrete gas that is carrying a net angular momentum. As the black hole mass grows, its spin changes in strength and direction due to its gravito-magnetic coupling with the small-scale accretion disc. We find that the black hole spins loose memory of their initial orientation, as accretion torques suffice to align the spins with the angular momentum of their orbit on a short time-scale ($\lesssim$1–2 Myr). A residual off-set in the spin direction relative to the orbital angular momentum remains, at the level of $\lesssim 10°$ for the case of a cold disc, and $\lesssim 30°$ for a warmer disc. Alignment in a cooler disc is more effective due to the higher coherence of the accretion flow near each black hole that reflects the large-scale coherence of the disc's rotation. If the massive black holes coalesce preserving the spin directions set after formation of a Keplerian binary, the relic black hole resulting from their coalescence receives a relatively small gravitational recoil. The distribution of recoil velocities inferred from a simulated sample of massive black hole binaries has median $\lesssim 70 \, \mathrm{km \, s^{-1}}$, much smaller than the median resulting from an isotropic distribution of spins.

Key words: black hole physics – hydrodynamics – galaxies: evolution – galaxies: nuclei – galaxies: starburst.

1 INTRODUCTION

The massive black holes (MBHs) that we observe today in local spheroids (Ferrarese & Ford 2005, and references therein) are expected to have grown through a series of major accretion episodes in symbiosis with the growth of their host galaxies. Gas-rich major mergers may be at the heart of this joint evolution as they may explain the morphology of the hosts and at the same time account for the fuelling of the underlying MBHs (e.g. Di Matteo, Springel & Hernquist 2005, and references therein). In the currently favoured cold dark matter hierarchical cosmologies, galaxy mergers play indeed a key role in growing galaxies to their present sizes, and the coalescence of MBHs in binaries is therefore expected to be rel-

atively common (Menou, Haiman & Narayanan 2001; Volonteri, Haardt & Madau 2003).

Following a galaxy major merger, the pair of MBHs first interacts with stars (Begelman, Blandford & Rees 1980; Milosavljević & Merritt 2001) and gas (Mayer et al. 2007). The pair loses orbital angular momentum, and it is expected to harden progressively down to subparsec scales where emission of gravitational radiation drives the MBH inspiral down to coalescence. Depending on the properties of the coalescing binary, the pattern of the gravitational wave emission can be anisotropic, resulting in a non-zero recoil velocity (a 'kick') of the MBH remnant (Redmount & Rees 1989). Several attempts to compute analytically the strength of the kick have been undertaken (Peres 1962; Bekenstein 1973; Fitchett 1983; Fitchett & Detweiler 1984; Redmount & Rees 1989; Wiseman 1992; Favata, Hughes & Holz 2004; Blanchet, Qusailah & Will 2005; Damour & Gopakumar 2006; Schnittman & Buonanno 2007).

⋆ E-mail: mdotti@umich.edu

Recent numerical simulations of the coalescence of spinning MBHs in full general relativity have been able to calculate explicitly kick velocities for a series of different binary configurations. It is found that three parameters influence the magnitude of the gravitational recoil of the relic MBH: the binary mass ratio, the spins and the mutual orientation of the spins with respect to the orbital angular momentum. The recoil is largest, up to $4000 \, \mathrm{km \, s^{-1}}$, for nearly equal mass MBHs with large spins, when the spin vectors have opposite directions and are in the orbital plane (Campanelli et al. 2007). By contrast, recoils of $\lesssim 200 \, \mathrm{km \, s^{-1}}$ are imparted to the MBH remnant if the spins of the progenitors prior coalescence are orthogonal to their orbital plane.

Purely general relativistic (GR) effects (i.e. spin-orbit and spin-spin interactions) may produce low recoil configurations, when the MBH pairing is driven by gravitational wave emission. However, those GR effects depend strongly on the initial relative orientation of the MBH spins, and can result in low recoil configurations only for a small region of parameter space (Schnittman 2004; Herrmann et al. 2009; Lousto et al. 2009).

In gas-rich mergers between galaxies of comparable mass (i.e. major mergers), close binary MBHs form under the action of dynamical friction against the gaseous and stellar background (Mayer et al. 2007; Callegari et al. 2009; see Colpi & Dotti 2009 for a review). During their inspiral MBHs are surrounded by a dense cocoon of gas that drives their dynamical decay and provides fuel for the feeding of the holes (Dotti et al. 2007, 2009). Since matter carries angular momentum also the spin vector can change during the accretion process. The details of the dynamics may have a profound influence on the mass and spin evolution of the two MBHs, and thus on the recoil velocity of the MBH resulting from their coalescence, and this is matter of our concern in this paper.

The spin evolution during the MBH inspiral in a gas-rich merger remnant has many implications. Spins, prior to coalescence, influence the extent of the gravitational recoil, and so the retention of the relic MBH inside its host galaxy. Accordingly, the spin distribution of the coalescing binaries is critical as it determines the frequency of MBH retention in the host halo (Volonteri & Rees 2006; Volonteri 2007; Volonteri, Haardt & Gultekin 2008; Gultekin et al., in preparation). The magnitude of the MBH spins and their orientation relative to the orbit during mergers are also critical in shaping the stellar density profiles in ellipticals, as the kicked MBH moving on a return orbit can deposit its excess kinetic energy into the stellar background, causing the formation of stellar core (Boylan-Kolchin, Ma & Quataert 2004; Gualandris & Merritt 2008). A recoiling MBH can have an observational signature when moving across the host galaxy, creating an X-ray tail in the perturbed hot gas (Devecchi et al. 2009), an off-set active nucleus (Loeb 2007; Volonteri & Madau 2008), shocking the inner rim of the accretion disc (Lippai, Frei & Haiman 2008; Schnittman & Krolik 2008) or dragging a stellar cusp with peculiarly high velocity dispersion (Merritt, Schnittman & Komossa 2009). Furthermore, spin orientations have important implications for gravitational wave astronomy, and for using gravitational wave measurements to constrain the formation history of MBHs (Vecchio 2004; Lang & Hughes 2006; Berti & Volonteri 2008; Arun et al. 2009a,b).

Bogdanovic, Reynolds & Miller (2007) proposed a physical process that could *align* the MBH spins with the orbital angular momentum of the binary, thus leading to slow recoils for the MBH remnant. The key process for alignment is the presence of a coherent gas inflow. They speculate that accreting gas exerts gravitomagnetic torques that suffice to align the spins of both the MBHs

with the angular momentum of the large-scale gas flow in which the orbit is embedded.

Spin-disc alignment due to gravito-magnetic coupling has been studied by a number of authors in the case of isolated MBHs surrounded by their own discs (Bardeen & Petterson 1975; Natarajan & Pringle 1998; Scheuer & Feiler 1996; Martin, Pringle & Tout 2007; Perego et al. 2009). Here, we attempt to explore for the first time spin-disc alignment around MBH binaries. We expect low recoils when the spin-disc coupling is strong, i.e. when:

(i) the two MBHs accrete $\gtrsim 1$ per cent of their initial mass before the coalescence (Natarajan & Pringle 1998; Natarajan & Armitage 1999; Volonteri, Sikora & Lasota 2007; Perego et al. 2009);

(ii) the accreted gas carries angular momentum in a preferred direction, flowing on to each MBH along a preferential plane determined by the distribution of angular momentum of the gas in the environment of the MBH.

The first requirement can be fulfilled if the MBHs pair inside a dense, massive gaseous nuclear disc (Dotti et al. 2009), such as that predicted to form in remnants of gas-rich major mergers by Mayer et al. (2007). To constrain the second requirement, we analyse a set of 3D smooth particle hydrodynamics (SPH) simulations already discussed in Dotti et al. (2009). The high resolution of these simulations enables us to resolve the gravitational sphere of influence of each MBH during their inspiral inside the circumnuclear disc, and to map the distribution of angular momentum of the SPH particles in the MBH vicinity. MBHs are modelled as *sink* particles that can accrete gas particles, allowing us to constrain the amount of mass accreted on to each MBH, and the orientation of the MBH spins relative to the angular momentum of the accreted gas.

The paper is organized as follows: in Section 2, we focus on the SPH simulations, and describe the semi-analytical algorithm that evolves the MBH spins; in Section 3, we illustrate our results on the MBH alignment and our prediction for the recoil velocity of the MBH remnant; in Section 4, we present our conclusions.

2 NUMERICAL METHODS

2.1 SPH simulations

We follow the dynamics of MBH pairs in nuclear discs using numerical simulations run with the *N*-body/SPH code GADGET (Springel, Yoshida & White 2001), upgraded to include the accretion physics. The simulations discussed in this paper are the same as presented in Dotti et al. (2009). Here, we give a short summary of the initial conditions for the different runs. For a more detailed discussion, we defer the reader to Dotti et al. (2009).

In our models, two MBHs are placed in the plane of a massive circumnuclear gaseous disc, embedded in a larger stellar spheroid. The gaseous disc is modelled with $\approx 2 \times 10^6$ particles, has a total mass $M_{\mathrm{Disc}} = 10^8 \, \mathrm{M_\odot}$, and follows a Mestel surface density profile $\Sigma(R) \propto R^{-1}$, where R is the radial distance projected into the disc plane. The outer radius of the disc is 100 pc. The massive disc is rotationally supported in R and has a vertical thickness of 8 pc. The internal energy per unit mass of the SPH particles scales as $u(R) \propto R^{-2/3}$, where the value of the temperature at the outer radius of the disc has been set in order to have the Toomre parameter (Toomre 1964) $Q \geq 3$ everywhere, preventing the fragmentation of the disc (the average value of Q over the disc surface is ≈ 10). Gas is evolved assuming a polytropic equation of state with index $\gamma = 5/3$ or $\gamma = 7/5$. In the former case, the runs are denoted by 'H' and are termed 'hot' as the temperature is proportional to a higher

power of density than in the latter class of runs ('cold' cases, runs denoted by 'C'). The cold case has been shown to provide a good approximation to a gas of solar metallicity heated by a starburst (Spaans & Silk 2000; Klessen, Spaans & Jappsen 2007). The hot case instead corresponds to an adiabatic monoatomic gas, as if radiative cooling was completely suppressed during the merger, for example as a result of radiative heating after gas accretion on to the MBHs (Mayer et al. 2007).

The spheroidal component (bulge) is modelled with 10^5 collisionless particles, initially distributed as a Plummer sphere with a total mass $M_{Bulge}(=6.98M_{Disc})$. The mass of the bulge within 100 pc is five times the mass of the disc, as suggested by Downes & Solomon (1998).

The two MBHs (M_1 and M_2) are equal in mass ($M_{BH} = 4 \times 10^6\,M_\odot$). The initial separation of the MBHs is 50 pc. M_1, called primary for reference, is placed at rest at the centre of the circumnuclear disc. M_2, termed secondary, is moving on an initially eccentric ($e_0 \simeq 0.7$) counterrotating (retrograde MBH, 'R' runs) or corotating (prograde MBH, 'P' runs) orbit with respect to the circumnuclear disc. Given the large masses of the disc and the bulge, the dynamics of the moving MBH (M_2) is unaffected by the presence of M_1 until the MBHs form a gravitationally bound system.

We allow the gas particles to be accreted on to the MBHs if the following two criteria are fulfilled:

(i) the sum of the kinetic and internal energy of the gas particle is lower than b-times the modulus of its gravitational energy (all the energies are computed with respect to each MBH);

(ii) the total mass accreted per unit time on to the MBH every time-step is lower than the accretion rate corresponding to the Eddington luminosity (L_{Edd}) computed assuming a radiative efficiency (ϵ) of 10 per cent.

The parameter b is a constant that defines the degree at which a particle is bound to the MBH in order to be accreted. We set $b = 0.3$. Note that due to the nature of the above criteria, the gas particles can accrete on to the MBHs only if the time-varying Bondi–Hoyle–Lyttleton radius is resolved in the simulations.

Each gas particle accreted by the MBH carries with it angular momentum. From the properties of the accreted particles, we can compute, as a function of time, the mass accretion rate and the versor $\hat{l}_{edge}$, that defines the direction of the total angular momentum of the accreted particles.

This information can be gathered only by performing very high resolution simulations. The gravitational softening of the MBHs is 0.1 pc. The gravitational softening of the gas particles is set to the same value, in order to prevent numerical errors. This is also the spatial resolution of the hydrodynamical force in the highest density regions.[1] The gravitational softening of the collisionless particles forming the bulge is 1 pc, in order to prevent two body interactions between gas particles and artificially massive stars. The main input parameters of our simulations are summarized in Table 1.

2.2 Semi-analytical Bardeen–Petterson effect

We use the MBH accretion histories obtained from our SPH simulations to follow the evolution of each MBH spin vector, $\boldsymbol{J}_{BH} = (aGM_{BH}^2/c)\hat{\boldsymbol{J}}_{BH}$, where $0 \le a \le 1$ is the dimensionless spin parameter and $\hat{\boldsymbol{J}}_{BH}$ is the spin versor. The scheme we adopt to

---

[1] The code computes the density of each SPH particle averaging over $N_{neigh} = 32$ neighbours.

Table 1. Run parameters.

Run	Prograde ?	e_0	γ
HP	Yes	0.7	5/3, 'hot'
HR	No	0.7	5/3, 'hot'
CP	Yes	0.7	7/5, 'cold'
CR	No	0.7	7/5, 'cold'

study the spin evolution is based on the model recently developed by Perego et al. (2009). Here, we summarize this algorithm.

We assume that during any accretion event recorded in our SPH simulations, the inflowing gas forms a geometrically thin/optically thick α-disc (Shakura & Sunyaev 1973) on milli-parsec scales (not resolved in the simulation), and that the outer disc orientation is defined by the unit vector $\boldsymbol{l}_{edge}$. The evolution of the α-disc is related to the radial viscosity ν_1 and the vertical viscosity ν_2 : ν_1 is the standard radial shear viscosity while ν_2 is the vertical shear viscosity associated to the diffusion of vertical warps through the disc. The two viscosities can be described in terms of two different dimensionless viscosity parameters, α_1 and α_2, through the relations $\nu_{1,2} = \alpha_{1,2}Hc_s$, where H is the disc vertical scale height and c_s is the sound speed of the gas in the accretion disc. We further assume $\alpha_2 = f_2/(2\alpha_1)$, with $\alpha_1 = 0.1$ and $f_2 = 0.6$ (Lodato & Pringle 2007). We assume power-law profiles for the two viscosities, $\nu_{1,2} \propto R^{3/4}$, as in the Shakura & Sunyaev solution.

As shown by Bardeen & Petterson (1975), if the orbital angular momentum of the disc around the MBH is misaligned with respect to the MBH spin, the coupled action of viscosity and relativistic Lense–Thirring precession warps the disc in its innermost region forcing the fluid to rotate in the equatorial plane of the spinning MBH. The time-scale of propagation of the warp is short compared with the viscous/accretion time-scale so that the deformed disc reaches an equilibrium profile that can be computed by solving the equation

$$\frac{1}{R}\frac{\partial}{\partial R}(RLv_R) = \frac{1}{R}\frac{\partial}{\partial R}\left(\nu_1 \Sigma R^3 \frac{d\Omega}{dR}\hat{l}\right) + \frac{1}{R}\frac{\partial}{\partial R}\left(\frac{1}{2}\nu_2 RL\frac{\partial \hat{l}}{\partial R}\right) + \frac{2G}{c^2}\frac{\boldsymbol{J}_{BH} \times \boldsymbol{L}}{R^3}, \quad (1)$$

where v_R is the radial drift velocity, Σ is the surface density, and Ω is the Keplerian velocity of the gas in the disc. $\boldsymbol{L}$ is the local angular momentum surface density of the disc, defined by its modulus L and the versor $\hat{l}$ that defines its direction.

The boundary conditions to equation (1) are the direction of $\boldsymbol{L}$ at the outer edge $\hat{l}_{edge}$, the mass accretion rate (that fixes the magnitude of Σ), and the values of mass and spin of each MBH. All these values but the MBH spins are directly obtained from the SPH runs. In particular, the direction of the unit vector $\hat{l}_{edge}$ is computed considering those SPH particles nearing the MBH gravitational sphere of influence that are accreted according to the criteria outlined in Section 2.1.

Also the MBH spin changes, not only because of accretion, but in response to its gravito-magnetic interaction with the disc on a time-scale longer than the time-scale of warp propagation (Perego et al. 2009). This interaction tends to reduce the degree of misalignment between the disc and the MBH spin, decreasing with time the angle between $\boldsymbol{J}_{BH}$ and $\hat{l}_{edge}$. The MBH spin evolution is followed by solving the equation:

$$\frac{d\boldsymbol{J}_{BH}}{dt} = \dot{M}\Lambda(R_{ISO})\hat{l}(R_{ISO}) + \frac{4\pi G}{c^2}\int_{disc}\frac{\boldsymbol{L} \times \boldsymbol{J}_{BH}}{R^2}dR. \quad (2)$$

The first term in equation (2) accounts for the angular momentum deposited on to the MBH by the accreted particles at the innermost stable orbit (ISO), where $\Lambda(R_{ISO})$ denotes the specific angular momentum at R_{ISO} and $\hat{l}(R_{ISO})$ the unit vector parallel to $\boldsymbol{J}_{BH}$, describing the warped disc according to the Bardeen–Petterson effect. The second term instead accounts for the gravo-magnetic interaction of the MBH spin with the warped disc. It modifies only the MBH spin direction (and not its modulus), conserving the total angular momentum of the composite (MBH+disc) system (King et al. 2005). The integrand in equation (2) peaks at the warp radius (R_{warp}) where the disc deformation is the largest.[2] Equation (2) incorporates two time-scales: the accretion time related to the first right-hand term describing the e-folding increase of the spin modulus, and the shorter time-scale of MBH spin alignment (Perego et al. 2009),

$$\tau_{al} \sim 10^5 a^{5/7} \left(\frac{M_{BH}}{4 \times 10^6 \, M_\odot} \right)^{-2/35} f_{Edd}^{-32/35} \, \text{yr}, \qquad (3)$$

that will ensure a high degree of MBH-disc gravito-magnetic coupling during MBH inspiral, as we will show promptly in Section 3. In equation (3), f_{Edd} is the MBH luminosity in units of L_{Edd}.

We applied iteratively equations (1) and (2) using inputs from the SPH simulation that give the values of the mass accretion rate, the MBH mass and the direction of $\hat{l}_{edge}$. The algorithm returns, as output, the spin vector, that is its magnitude and direction. At each time-step, our code therefore provides the angle between the spin vector of each MBH and the angular momentum vector of their relative orbit.

3 RESULTS

Fig. 1 shows the time evolution of the relative angle θ between the spin of each MBH and the orbital angular momentum of the MBH pair ($\boldsymbol{L}_{pair} = L_{orb}\hat{l}_{pair}$), for two selected runs (CP and HR). The initial relative angle (θ_i) has been arbitrarily set to 2.5 rad (143°), while a has initially five different values (0.2, 0.4, 0.6, 0.8 and 1).

There is a common trend in all the runs for both MBHs: MBHs with lower spins tend to align faster (as shown in Fig. 1 for $t \lesssim 2$–4 Myr) and are affected by changes in the plane of the accreting material to a larger extent (θ changes rapidly with time and has more pronounced minima/maxima for lower a, see again Fig. 1). As indicated by equation (3), a smaller spin modulus implies a shorter alignment time, and this explains the faster response of the MBH to orient its spin orthogonal to the plane of the accreted gas. A slowly spinning MBH induces a weaker warp in the disc: the warp radius decreases with decreasing a and there the Lense–Thirring precession time is faster so that the MBH is more responsive to changes in the orientation of the accreted gas (see Perego et al. 2009 for details).

The spin evolution depends also on the dynamical properties of the MBHs and on the thermodynamics of the circumnuclear disc. The effect of the initial orbital parameters is important during the first phase of orbital decay of the two MBHs, before they form a binary. We consider the two MBHs to be bound in a binary if the mass in gas and stars inside their orbits is lower than the mass of the binary. This happens when the separation between the two MBHs

Figure 1. Upper panels: time evolution of the relative angle between M_2 spin and the orbital angular momentum of the MBH pair. Left-hand (right-hand) panel refers to runs CP (HR). The initial angle is arbitrarily set to 2.5 rad (close to anti-aligned), and the initial spin parameter magnitudes varies between 0.2 (lighter colours) to 1 (darker colours). Lower panels: same as upper panels for M_1.

Table 2. Third column: MBH binary formation time. Fourth column: component parallel to $\boldsymbol{L}_{pair}$ of the angular momentum of the gas particles accreted after the formation of the binary (ΔL_z), normalized to its modulus (ΔL). Fifth column: average value of the angle between the MBH spins and $\boldsymbol{L}_{pair}$, after the formation of a binary.

Run	MBH	t_{bin} (Myr)	$\Delta L_z/\Delta L$	θ_f (rad)
CP	M_1	6.5	>99.9 pre cent	0.10
CP	M_2	6.5	>99.9 pre cent	0.13
CR	M_1	4.5	>99.9 pre cent	0.15
CR	M_2	4.5	>99.9 pre cent	0.16
HP	M_1	7.5	96.3 pre cent	0.25
HP	M_2	7.5	94.9 pre cent	0.23
HR	M_1	4.5	81.9 pre cent	0.42
HR	M_2	4.5	77.9 pre cent	0.32

is ≈ 5 pc. The time at which the two MBHs form a binary (t_{bin}) is reported in Table 2 for each run. As described in detail in Section 3.1, M_2 loses memory of its initial orbital parameters before binding in a binary. As a consequence, the properties of accreting gas on to the MBHs after the formation of the binary are almost independent of the initial dynamical parameters of the pair. At this late stage of the orbital evolution, the gas accretion rate and the coherence of the accretion flows depend mostly on the thermodynamics of the circumnuclear disc. Summarizing, for $t < t_{bin}$ both dynamical and thermodynamical properties affect spin evolution, while for $t > t_{bin}$ the thermodynamical properties ultimately determine the final degree of spin alignment.

---

[2]The exact definition of R_{warp} is where the vertical viscous time R^2/ν_2 in the disc is comparable to the Lense–Thirring precession time. Because R_{warp} and the radius at which the disc is maximally deformed are comparable (Perego et al. 2009), we simplify the notation in the paper using only R_{warp}.
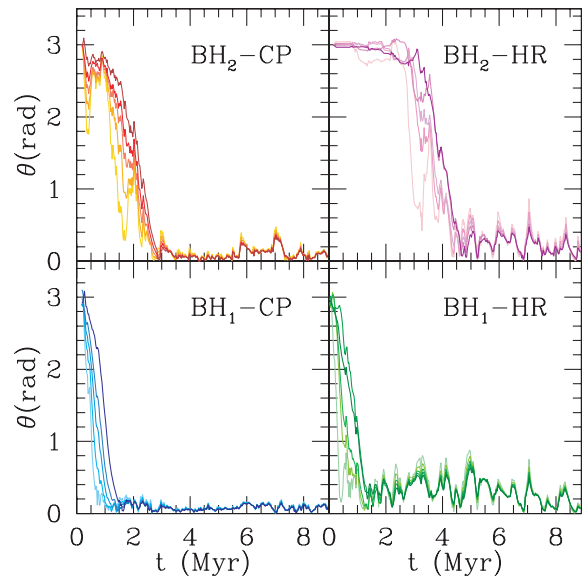
3.1 Effects of dynamics on spin alignment

We note that for each MBH and every run, θ initially ($t < 4.5$ Myr) decreases with time, but the alignment process is more efficient for M_1 in both simulations. This delay in the alignment of M_2 is related to the orbital evolution of the orbiting MBH. In runs CP and HP, M_2 is initially corotating with the circumnuclear disc on an eccentric orbit. Because of the eccentricity of the orbit, M_2 has a non-zero relative velocity with respect to its local gas environment. As a consequence, the accretion rate on to M_2 is initially lower than accretion rate on to M_1 (Dotti et al. 2009). Dynamical friction exerted by the circumnuclear disc on to the orbiting MBH circularizes the orbit of M_2 before the formation of a binary (Dotti, Colpi & Haardt 2006a; Dotti et al. 2007), so that the relative velocity between gas particles and M_2 decreases. After dynamical friction circularized the orbit of M_2, the accretion rate on to M_2 increases and becomes comparable to the accretion rate on to M_1 (Dotti et al. 2009). As a consequence the alignment of the spin of M_2 becomes more efficient, and by the time a binary forms, θ has similar values for M_1 and M_2 in the same run.

For initially counterrotating MBHs (runs HR and CR), the effect of the dynamics on to the spin evolution of M_2 is more pronounced. Dynamical friction drags the orbiting MBH in the direction of the rotating gas, so that, before the formation of a binary, M_2 starts to corotate with respect to the circumnuclear disc ('orbital angular momentum flip'; Dotti et al. 2009). In the counterrotating runs, the ratio between the accretion rate on to M_2 before and after the angular momentum flip can be $\lesssim 0.15$. As a consequence, during the first 2–3 Myr, when the secondary moves on a retrograde orbit, θ does not change significantly (because of the low accretion rate), while it decreases efficiently only after the orbital angular momentum flip.

3.2 Effects of gas thermodynamics on spin alignment

Alignment occurs over a short time-scale, as indicated by the steep drop of θ in Fig. 1. Afterwards, θ starts to oscillate around an average value, different from run to run. Numerical noise due to the discrete nature of SPH calculations does not affect these oscillations. During each oscillation, the MBHs accrete tens of $N_{\rm neigh}$. In particular, the average value of θ and the amplitude of its oscillations are in general larger for hot runs (see Fig. 1). We define $\theta_{\rm f}$ as the angle between the MBH spins and $\mathbf{L}_{\rm pair}$ after the formation of a binary [$\theta_{\rm f} = \theta(t > t_{\rm bin})$]. This new parameter is of key importance in the following discussion, since we assume that the distribution of $\theta_{\rm f}$ is representative of θ at coalescence. The validity of this assumption is discussed in Section 3.3.

The last column of Table 2 shows the average value of $\theta_{\rm f}$ of each MBH in every run. We note that $\theta_{\rm f}$ is lower when the MBHs are embedded in colder discs. This is due to the properties of gas close to each MBH. For larger γ (hot runs), the temperature of the gas in the overdense regions around each MBH is higher, and so is the pressure. As a consequence, the gas structures around each MBH (and the gas particles accreting on to the MBHs) are more pressure supported, spherical distributed, and with more isotropic velocities in runs HP and HR, while gas is more rotationally supported in runs CP and CR. This effect is quantified in Table 2. In the fourth column, we report the component parallel to $\mathbf{L}_{\rm pair}$ of the angular momentum of the gas particles accreted after the formation of the binary (ΔL_z), normalized to its modulus (ΔL). In cold runs, after the formation of the binary, streams of gas accreting on to the MBHs are extremely coherent ($\Delta L_z/\Delta L > 99.9$ per cent). In hot runs, the accreting particles have a larger degree of isotropy, resulting in less coherent accretion processes ($\Delta L_z/\Delta L \lesssim 95$ per cent) and larger/more variable $\theta_{\rm f}$.

Since the time when a binary forms ($t_{\rm bin}$) is different for different runs, the time intervals (Δt) over which we average $\theta_{\rm f}$ are different. We decided to keep constant Δt for runs with the same polytropic index, but we used different Δt for cold and hot runs, in order to maximize the statistic. We chose $\Delta t = 3.5$ Myr for runs PC and RC, and $\Delta t = 1$ Myr for runs PH and RH. Averaging over different times does not affect the main results discussed above. As a check, we computed $\theta_{\rm f}$ and Δt for the two MBHs in runs PC and RC averaging over only 1 Myr, and for every MBH/cold run combination we find $\theta_{\rm f} < 0.19\,(10°)$ and $\Delta L_z/\Delta L > 99$ per cent, consistent with the values reported in Table 2 for $\Delta t = 3.5$ Myr.

We also note that physical processes not implemented in these simulations, such as star formation or feedback from supernovae, could decrease the degree of coherency of the accreting gas, possibly resulting in higher $\theta_{\rm f}$. Furthermore, Lodato et al. 2009 have shown that star formation depletes the reservoir of gas in the vicinity of the MBHs, and can slow down the decay of the binary at subparsec separations. A detailed study of the interaction between star formation in the circumnuclear disc and the properties of the accreting gas is postponed to a future investigation.

We estimated the efficiency of the alignment process over a large Monte Carlo sample of initial $\mathbf{J}_{\rm BH}$. For each MBH and each run, we selected 20 000 different initial values of a, homogeneously distributed between 0 and 1. For each value of a, we computed the three components of $\mathbf{J}_{\rm BH}$, assuming an initially isotropic distribution of the spins. We evolved the initial condition for $\mathbf{J}_{\rm BH}$ using the outputs of our simulations, as described in Section 2.2. As already discussed in Section 3, the degree of alignment between MBH spins and $\mathbf{L}_{\rm pair}$ at $t > t_{\rm bin}$ is ultimately determined by the gas thermodynamics. As a consequence, we do not further analyse the dependence on the initial dynamics of M_2, and focus mainly on the effect of the disc thermodynamics. The results from runs CP and CR have been combined in a single class (left-hand panels in Fig. 2). The same has been done for runs HP and HR (right-hand panels in Fig. 2).

Fig. 2 shows the density of realizations obtained with our statistical analysis, in the ($\theta_{\rm i}$; $\theta_{\rm f}$) plane. Dark, medium and light-grey surfaces refer to regions of decreasing density, encompassing 68.3, 95.5 and 99.7 per cent of the realizations. We note that the alignment process is efficient independently of $\theta_{\rm i}$. The lower density for $\theta_{\rm i} \approx 0$ and π is due to the initial isotropic distribution of the spins, and is totally unrelated to the alignment process. As already discussed above, alignment is more efficient for MBHs in cold discs. In these runs (left-hand panels of Fig. 2), 68.3 per cent of the realizations have a final angle between the two MBHs and the orbital angular momentum of the pair $\theta_{\rm f} \lesssim 0.1\,(6°)$ while 68.3 per cent of the realizations in runs HP and HR have $\theta_{\rm f} \lesssim 0.5\,(29°)$. There are a few per cent of the realizations with 'large' final angles [$\theta_{\rm f} \gtrsim 0.5\,(29°)$] in every run.

3.3 Recoil distributions

In this section, we assume that the two MBHs can reach coalescence, and we use the distributions of $\theta_{\rm f}$ for M_1 and M_2 shown in Fig. 2 in order to compute distributions of recoil velocities for the MBH remnant. We assume also that the distributions of $\theta_{\rm f}$ obtained are representative of the relative angle between the MBH spins and $\mathbf{L}_{\rm pair}$ during last phase of orbital decay, when the two MBHs lose efficiently orbital energy and angular momentum due to the gravitational wave emission. These assumptions are necessary because our simulations (spatial resolution ≈ 0.1 pc) cannot follow
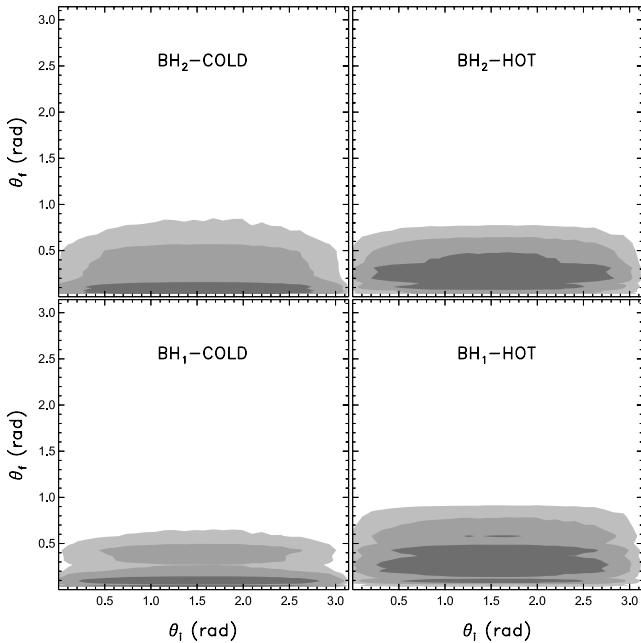
Figure 2. Density distribution of pairs $(\theta_i; \theta_f)$ of the initial/final relative angles between MBH spins and orbital angular momentum. Left- and right-hand panels refer to MBHs embedded in cold and hot discs, respectively. Upper (lower) panels refer to the spin of M_2 (M_1). Dark, medium and light-grey surfaces refer to high-density regions encompassing 68.3, 95.5 and 99.7 per cent of the realizations. θ_i has been sampled isotropically, and the dimensionless spin parameters (a) have been sampled from a constant probability distribution, between 0 and 1. As discussed in the text, we average θ_f over all the times after the formation of the MBH binary.
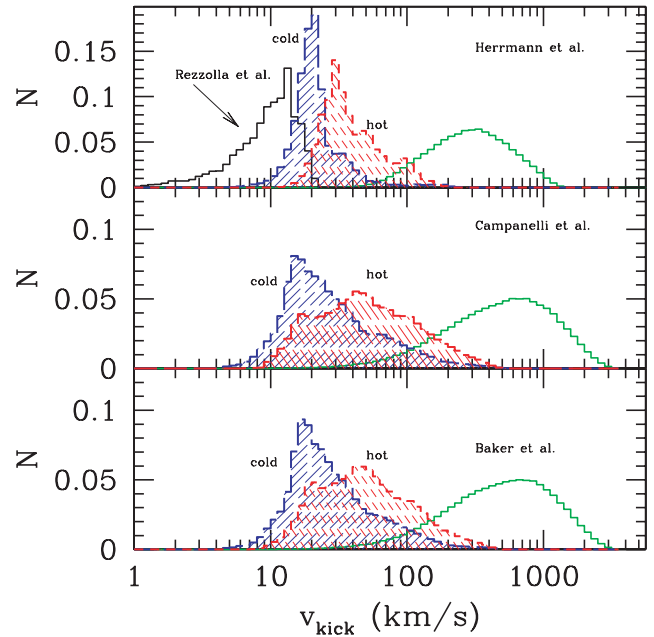

Figure 3. Distribution of recoil velocities. The blue (red) histogram is computed from the distribution of spins we obtain from our simulations, after the alignment of the spins in a cold (hot) circumnuclear disc. The green curves refer to recoil velocities obtained assuming the spins of the two MBHs to be isotropically distributed. Upper, middle and lower panels refer to the results obtained using fit H, fit CL and fit B, respectively. In the upper panel, the black histogram shows as a comparison the distribution of recoil velocity obtained using fit R, assuming complete alignment between the MBH spins and L_{pair}. In this case, both the results of cold and hot runs have been considered in a single histogram. In all the histograms, the mass ratio between the MBHs (q) is obtained from our SPH simulations.

the evolution of the MBHs down to separations where gravitational waves dominate the dynamics. The two assumptions are valid if one of the following requirements is fulfilled.

(i) The gas accretes on to the two MBHs in a coherent way until star formation and/or AGN feedback deplete the galactic nucleus of gas, and no further accretion events (i.e. due to tidal stripping of stars) change significantly the direction of the MBH spins.

(ii) The dynamical interaction between the binary and the gas creates a low-density region (the so-called 'gap'; Gould & Rix 2000), reducing/halting accretion on to the MBHs (Milosavljevic & Phinney 2005; Dotti et al. 2006b; Hayasaki, Mineshige & Sudou 2007; Cuadra et al. 2009) so that the spins of the two MBHs do not change significantly when the binary separation is $\lesssim 0.1$ pc;

(iii) After forming a binary, the two MBH can reach the final coalescence in a short time ($\lesssim 10$ Myr), so that further accretion events do not have time to change significantly the MBH spin orientations.

Numerical GR computations show that the recoil velocity V_{kick} depends on the binary mass ratio $q = M_2/M_1$, on the dimensionless spin vectors of the pair a_1 and $a_2 (0 < a_i < 1)$, and on the orbital parameters. This information can be obtained from the analysis of our simulations. We use four different prescriptions from the literature to compute the recoil velocity of the MBH remnant, based on Campanelli et al. (2007) and Lousto & Zlochower (2009; fit CL), Baker et al. (2008; fit B), Herrmann et al. (2007; fit H) and Rezzolla et al. (2008; fit R).

We use fit R as a consistency check, as this formula provides the recoil velocity for completely aligned configurations (θ_f from the simulations is close to, but not exactly zero), yielding lower limits

for V_{kick}. When using fit R we adopt the spin magnitudes obtained from our simulations, further assuming that MBH spins are fully aligned with L_{pair} at coalescence, and $q = 1$.[3] Expressions of the fitting formulae are detailed in the Appendix.

The distributions of recoil velocities we obtain for cold (blue histograms) and hot (red histograms) discs are shown in Fig. 3. For these three fitting formulae, we report the distribution of recoil velocities we would obtain assuming that the MBH spins are isotropically distributed (green lines). Because of the spin alignment discussed in Sections 3.2 and 3.3, the recoil velocities we obtain analysing the results of our simulations are approximately one order of magnitude smaller than those predicted for isotropically distributed MBH spins, independently of the fitting formula we consider. Furthermore, the recoils obtained evolving the MBH pair in a cold circumnuclear disc are always a factor of ≈ 2 smaller than the velocities obtained in the hot cases. This shift is due to the lower level of alignment between MBH spins and L_{pair} for MBHs orbiting in hot discs, as discussed in Section 3.2. The mean values of recoil velocities for these three fitting formulae and for different gas thermodynamics are shown in the first two columns of Table 3. Because the mean values can be affected by the long tails of the recoil distributions at high velocities, we report also the median values in last two columns of the same table.

---

[3]The MBH mass ratio in our simulations is always between 0.9 and 1. Assuming $q = 1$ does not affect our results.

Table 3. Recoil statistics. All velocities are in $km\,s^{-1}$.

	Cold disc Mean	Hot disc Mean	Cold disc Median	Hot disc Median
Fit CL	40^{+50}_{-40}	62^{+42}_{-42}	23^{+13}_{-13}	51^{+32}_{-32}
Fit B	39^{+45}_{-39}	67^{+61}_{-61}	24^{+12}_{-12}	46^{+28}_{-28}
Fit H	33^{+27}_{-27}	54^{+33}_{-33}	23^{+7}_{-7}	41^{+16}_{-16}

Fit CL, fit B and fit H give similar mean and median values, consistent within a factor of ≈ 1–1.3. The fraction of remnants with recoils larger than in cold (hot) runs with recoils larger than 400 $km\,s^{-1}$ ('fast recoils') is 0.2 per cent (8 per cent) using fit CL. Fit B has the same fraction of fast recoils in cold runs, and a lower fraction (0.2 per cent) in cold runs. Fit H does not have any realization with such high recoils.

The black histogram in the upper panel shows the distributions of recoil velocities obtained using fit R. In this case, we considered both the results of cold and hot runs in a single histogram. Mean and median values for the recoils are ≈ 10 $km\,s^{-1}$. Such low values follow from using the distributions of a_i that we obtain from our simulations. After the formation of a binary, the MBHs in our runs have spin magnitudes $0.3 \lesssim a_i \lesssim 0.9$. If instead we assumed a homogeneous distribution of spins between 0 and 1, fit R would predict a kick distribution with a peak at ≈ 100 $km\,s^{-1}$, a sharp cut-off at higher velocities, and a long tail at lower values. As expected, fit R gives a lower limit for the recoil velocities. The recoil distribution obtained with this last prescription peaks at velocities which are only ≈ 2 times smaller than those where the cold runs peak, when using the other three fits. This confirms that these fitting formulae well describe quasi-aligned configurations.

4 DISCUSSION

In this paper, we traced for the first time the evolution of the spin vectors of MBHs orbiting inside a massive circumnuclear gas disc. Our SPH simulations have sufficiently high resolution to probe the hydrodynamics of fluid particles and the accretion physics near the gravitational sphere of influence of the MBHs. An ad hoc algorithm designed for tracking the gravo–magnetic coupling between the MBH spin and the small-scale accretion disc is then implemented in the code. We find that:

(i) when evolving a in dense, rotationally supported, structure such as a circumnuclear disc, MBHs in a pair align their spins ($J_{BH_{1,2}}$) to the pair orbital angular momentum (L_{pair}) well before the two MBHs bind in a Keplerian binary, and independently of the MBHs initial orbital parameters. For a run with M_2 initially on a retrograde orbit, the spin of the secondary aligns efficiently only after the 'orbital angular momentum flip';

(ii) the average angle between $J_{BH_{1,2}}$ and L_{pair} after the binary formation (θ_f) depends on the thermodynamics of the massive circumnuclear discs. θ_f is lower if the MBHs are embedded in colder discs (with a polytropic index $\gamma = 7/5$), with respect to hotter discs ($\gamma = 5/3$);

(iii) after the formation of a binary, the two MBHs accrete gas with the same dynamical and thermodynamical properties. As a consequence, even the angle between the two small projections of $J_{BH_{1,2}}$ in the orbital plane decreases. This further reduces the recoil velocity of the MBH remnant. The degree of alignment between the two spins and between each spin and L_{pair} is preserved (or even

increased) by spin–spin and spin–orbit interactions until the plunge phase (Schnittman 2004; Herrmann et al. 2009);

(iv) due to the efficient alignment between $J_{BH_{1,2}}$ and L_{pair}, the expected recoil velocities (V_{kick}) at the MBH coalescence are, on average, one order of magnitude lower than those expected for randomly oriented MBH spins. The thermodynamical properties of the environment affect the degree of alignment and, as a consequence, the expected recoil velocities. V_{kick} is lower (by a factor of 1.5–2.2) for lower values of γ;

(v) assuming the same distribution of θ_f, the recoil velocity distributions obtained using different prescriptions are very similar. The three fitting formulae used predict the same mean and median recoil velocities ($\lesssim 70\,km\,s^{-1}$) within a factor of ≈ 1–1.3, with less than few percent of realizations having $V_{kick} > 400$ $km\,s^{-1}$.

The distributions of recoil velocities that we find have important consequences for retention of MBHs in galactic nuclei. When MBH binaries form and evolve in gas-rich major mergers, we predict the recoil velocity to be, on average, well below the escape speed from low-redshift galaxies. Indeed, because of the extreme efficiency of the spin alignment process, the recoil velocities are likely unimportant even for high-z proto-galactic building blocks. Volonteri & Rees (2006) and Volonteri (2007) discussed how strong recoils can affect the early growth of MBHs at the highest redshifts. In a forthcoming paper, we will update our calculations and determine the impact of low recoils on the growth of MBHs in galaxies.

Our simple treatment of thermodynamics and the absence of any prescription for star-formation and supernovae feedback in our simulations could, in principle, overestimate the degree of coherency in the gas flows accreting on to the MBHs. Furthermore, our finite resolution prevents us from studying the fragmentation of the accretion discs forming around the MBHs, that could result in a sequence of short and randomly oriented accretion events (King & Pringle 2006). We will investigate interaction between star formation in the circumnuclear disc and the properties of the accreting gas in a forthcoming study.

REFERENCES

Arun K. G. et al., 2009a, Class. Quantum Gravity, 26, 094027
Arun K. G., Buonanno A., Faye G., Ochsner E., 2009b, Phys. Rev. D, 79, 104023
Baker J. G., Boggs W. D., Centrella J., Kelly B. J., McWilliams S. T., Miller M. C., van Meter J. R., 2008, ApJ, 682, L29
Bardeen J. M., Petterson J. A., 1975, ApJ, 195, L65
Begelman M. C., Blandford R. D., Rees M. J., 1980, Nat, 287, 307
Bekenstein J. D., 1973, ApJ, 183, 657
Berti E., Volonteri M., 2008, ApJ, 684, 822
Blanchet L., Qusailah M. S. S., Will C. M., 2005, ApJ, 635, 508
Bogdanovic T., Reynolds C. S., Miller M. C., 2007, ApJ, 661, L147
Boylan-Kolchin M., Ma C. P., Quataert E., 2004, ApJ, 613, L37

Callegari S., Mayer L., Kazantzidis S., Colpi M., Governato F., Quinn T., Wadsley J., 2009, ApJ, 696, L89

Campanelli M., Lousto C. O., Zlochower Y., Merritt D., 2007, ApJ, 659, L5

Colpi M., Dotti M., 2009, Adv. Sci. Lett., in press (arXiv:0906.4339)

Cuadra J., Armitage P. J., Alexander R. D., Begelman M. C., 2009, MNRAS, 393, 1423

Damour T., Gopakumar A., 2006, Phys. Rev. D, 73, 124006

Devecchi B., Rasia E., Dotti M., Volonteri M., Colpi M., 2009, MNRAS, 394, 633

Di Matteo T., Springel V., Hernquist L., 2005, Nat, 2005, 433, 604

Dotti M., Colpi M., Haardt F., 2006a, MNRAS, 367, 103

Dotti M., Salvaterra R., Sesana A., Colpi M., Haardt F., 2006b, MNRAS, 372, 869

Dotti M., Colpi M., Haardt F., Mayer L., 2007, MNRAS, 379, 956

Dotti M., Ruszkowski M., Paredi L., Colpi M., Volonteri M., Haardt F., 2009, MNRAS, 396, 1640

Downes D., Solomon P. M., 1998, ApJ, 507, 615

Favata M., Hughes S. A., Holz D. E., 2004, ApJ, 607, L5

Ferrarese L., Ford H., 2005, Space Sci. Rev., 116, 523

Fitchett M. J., 1983, MNRAS, 203, 1049

Fitchett M. J., Detweiler S., 1984, MNRAS, 211, 933

Gould A., Rix H. W., 2000, ApJ, 532, L29

Gualandris A., Merritt D., 2008, ApJ, 678, 780

Hayasaki K., Mineshige S., Sudou H., 2007, PASJ, 59, 427

Herrmann F., Hinder I., Shoemaker D. M., Laguna P., Matzner R. A., 2007, Phys. Rev. D, 76, 084032

Herrmann F., Silberholz J., Bellone M., Guerberoff G., Tiglio M., 2009, preprint (arXiv:0908.3889)

King A. R., Pringle J. E., 2006, MNRAS, 373, L90

King A. R., Lubow S. H., Ogilvie G. I., Pringle J. E., 2005, MNRAS, 363, 49

Klessen R. S., Spaans M., Jappsen A., 2007, MNRAS, 374, L29

Lang R. N., Hughes S. A., 2006, Phys. Rev. D, 74, 122001

Lippai Z., Frei Z., Haiman Z., 2008, ApJ, 676, L5

Lodato G., Pringle J. E., 2007, MNRAS, 381, 1287

Lodato G., Nayakshin S., King A. R., Pringle J. E., 2009, MNRAS, 398, 1392

Loeb A., 2007, Phys. Rev. Lett., 99, 041103

Lousto C. O., Zlochower Y., 2009, Phys. Rev. D, 79, 064018

Lousto C. O., Nakano H., Zlochower Y., Campanelli M., 2009, preprint (arXiv:0910.3197)

Martin R. G., Pringle J. E., Tout C. A., 2007, MNRAS, 381, 1617

Mayer L., Kazantzidis S., Madau P., Colpi M., Quinn T., Wadsley J., 2007, Sci, 316, 1874

Menou K., Haiman Z., Narayanan V. K., 2001, ApJ, 558, 535

Merritt D., Schnittman J. D., Komossa S., 2009, ApJ, 699, 1690

Milosavljević M., Merritt D., 2001, ApJ, 563, 34

Milosavljevic M., Phinney E. S., 2005, ApJ, 622, L93

Natarajan P., Armitage P. J., 1999, MNRAS, 309, 961

Natarajan P., Pringle J. E., 1998, ApJ, 506, L97

Perego A., Dotti M., Colpi M., Volonteri M., 2009, MNRAS, 399, 2249

Peres A., 1962, Phys. Rev., 128, 2471

Rezzolla L., Dorband E. N., Reisswig C., Diener P., Pollney D., Schnetter E., Szilagyi B., 2008, ApJ, 679, 1422

Scheuer P. A. G., Feiler R., 1996, MNRAS, 282, 291

Schnittman J. D., 2004, Phys. Rev. D, 70, 124020

Schnittman J. D., Buonanno A., 2007, ApJ, 662, L63

Schnittman J. D., Krolik J. H., 2008, ApJ, 684, 870

Shakura N. I., Sunyaev R. A., 1973, A&A, 24, 337

Spaans M., Silk J., 2000, ApJ, 538, 115

Springel V., Yoshida N., White S. D. M., 2001, New Astron., 6, 79

Redmount I. H., Rees M. J., 1989, Comments Astrophys., 14, 165

Toomre A., 1964, ApJ, 139, 1217

Vecchio A., 2004, Phys.Rev. D, 70, 042001

Volonteri M., 2007, ApJ, 663, L5

Volonteri M., Madau P., 2008, ApJ, 687, L57

Volonteri M., Rees M. J., 2006, ApJ, 650, 669

Volonteri M., Haardt F., Madau P., 2003, ApJ, 582, 559

Volonteri M., Sikora M., Lasota J.-P., 2007, ApJ, 667, 704

Volonteri M., Haardt F., Gultekin K., 2008, MNRAS, 384, 1387

Wiseman A. G., 1992, Phys. Rev. D, 46, 1517

APPENDIX A: FITTING FORMULAE FOR RECOIL VELOCITIES

Campanelli et al. (2007) and Lousto & Zlochower (2009; fit CL) propose the following fitting formula for the post-coalescence recoil of a MBH remnant:

$$V_{kick} = \sqrt{v_m^2 + v_\perp^2 + 2 v_m v_\perp \cos(\xi) + v_\parallel^2}, \tag{A1}$$

$$v_m = A\eta^2 \sqrt{1 - 4\eta}\,(1 + B\eta), \tag{A2}$$

$$v_\perp = \frac{H\eta^2}{(1+q)}\left(a_1^\parallel - q a_2^\parallel\right), \tag{A3}$$

$$v_\parallel = \frac{K\eta^2}{(1+q)}\cos(\Theta - \Theta_0)|\boldsymbol{a}_1^\perp - q\boldsymbol{a}_2^\perp|, \tag{A4}$$

where $A = 1.2 \times 10^4 \,\mathrm{km\,s^{-1}}$, $B = -0.93$, $H = 6900 \,\mathrm{km\,s^{-1}}$, $K = 6.0 \times 10^4 \,\mathrm{km\,s^{-1}}$, $\eta \equiv q/(1+q)^2$ is the symmetric mass ratio and ξ measures the angle between the unequal mass and the spin contribution to the recoil velocity in the orbital plane. We assumed $\xi = 145°$, as suggested by Lousto & Zlochower. The components of the spins of the two MBHs are

$$a_1^\perp = a_1 \sin(\theta_1),$$
$$a_1^\parallel = a_1 \cos(\theta_1),$$
$$a_2^\perp = a_2 \sin(\theta_2),$$
$$a_2^\parallel = a_2 \cos(\theta_2),$$

where the indices $\parallel$ and $\perp$ refer to projections parallel and perpendicular to the orbital angular momentum, respectively, and $\theta_1(\theta_2)$ refers to θ_f for the primary (secondary) MBH. In equation (A4), Θ is the angle between $(\boldsymbol{a}_2^\perp - q\,\boldsymbol{a}_1^\perp)$ and the separation vector at coalescence, and Θ_0 depends on the initial separation between the holes. Since Θ_0 is unknown, for this exploration we assume a flat distribution of $\Theta - \Theta_0$ between 0 and 2π.

Baker et al. (2008; fit B) propose instead the following fitting formula for $v_\parallel$:

$$v_\parallel = \frac{K\eta^3}{(1+q)}[a_1^\perp \cos(\phi_1 - \Phi_1) - q a_2^\perp \cos(\phi_2 - \Phi_2)], \tag{A5}$$

where $\phi_1(\phi_2)$ is the angle between $a_1^\perp$ ($a_2^\perp$) and a fixed reference direction. Following Baker et al. (2008), $\Phi_1 = \Phi(q)$ and $\Phi_2 = \Phi(1/q)$. Because in our simulations $q \approx 1$, we fixed $\Phi_1 = \Phi_2$. We further assume a flat distribution of Φ_1 between 0 and 2π. In this case, $A = 1.35 \times 10^4 \,\mathrm{km\,s^{-1}}$, $B = -1.48$, $H = 7540 \,\mathrm{km\,s^{-1}}$ and $K = 2.4 \times 10^5 \,\mathrm{km\,s^{-1}}$.

Herrmann et al. (2007; fit H) formulate the recoil velocity of a MBH remnant as a function of a different angle θ_H, i.e. the angle between $\boldsymbol{L}_{pair}$ and

$$\boldsymbol{\Sigma} = M\left(\frac{\boldsymbol{J}_2}{M_2} - \frac{\boldsymbol{J}_1}{M_1}\right), \tag{A6}$$

where $M = M_1 + M_2$. Assuming that $\boldsymbol{L}_{pair}$ is aligned with the z direction, they find that the Cartesian component of the recoil velocity follow

$$V_x = C_0 H_x \cos(\theta_H), \tag{A7}$$

$$V_y = C_0 H_y \cos(\theta_H), \tag{A8}$$

$$V_z = C_0 K_z \sin(\theta_H), \tag{A9}$$

where $C_0 = \Sigma\, q^2/[M^2(1+q)^4]$, and the best-fitting parameters are $H_x = 2.1 \times 10^3$ $H_y = 7.3 \times 10^3$, and $K_z = 2.1 \times 10^4$.[4]

---

[4]The values of H_x, H_y and K_z published in Herrmann et al. (2007) contain a typo (Laguna, private communication).

The last fitting formula we use to compute V_{kick} has been proposed by Rezzolla et al. (2008; fit R). In their study, they consider only equal-mass MBHs with spins aligned with $\boldsymbol{L}_{pair}$. They find

$$V_{kick} = |c_1(a_1 - a_2) + c_2(a_1^2 - a_2^2)|, \tag{A10}$$

where $c_1 = -220.97$ and $c_2 = 45.52$. Equation (A10) provides recoil velocities for completely aligned configurations.

This paper has been typeset from a TeX/LaTeX file prepared by the author.